PERGAMON

Brief paper

Stable polyhedra in parameter space [☆]

Jürgen Ackermann*, Dieter Kaesbauer

German Aerospace Center, DLR Oberpfaffenhofen, Institute of Robotics and Mechatronics, D-82234 Wessling, Germany

Abstract

A typical uncertainty structure of a characteristic polynomial is $P(s) = A(s)Q(s) + B(s)$ with $A(s)$ and $B(s)$ fixed and $Q(s)$ uncertain. In robust controller design $Q(s)$ may be a controller numerator or denominator polynomial; an example is the PID controller with $Q(s) = K_I + K_P s + K_D s^2$. In robustness analysis $Q(s)$ may describe a plant uncertainty. For fixed imaginary part of $Q(j\omega)$, it is shown that Hurwitz stability boundaries in the parameter space of the even part of $Q(j\omega)$ are hyperplanes and the stability regions are convex polyhedra. A dual result holds for fixed real part of $Q(j\omega)$. Also σ-stability with the real parts of all roots of $P(s)$ smaller than σ is treated.

Under the above conditions, the roots of $P(s)$ can cross the imaginary axis only at a finite number of discrete "singular" frequencies. Each singular frequency generates a hyperplane as stability boundary. An application is robust controller design by simultaneous stabilization of several representatives of $A(s)$ and $B(s)$ by a PID controller. Geometrically, the intersection of convex polygons must be calculated and represented tomographically for a grid on K_P.
© 2003 Published by Elsevier Science Ltd.

Keywords: PID control; Robustness; Parameter space

1. Introduction

It has been shown (Ho, Datta, & Bhattacharya, 1998; Datta, Ho, & Bhattacharya, 2000) that stability regions of PID controllers with fixed proportional gains consist of convex polygons. The proof was given via a generalization of the Hermite–Biehler theorem. An alternative proof was given more recently (Munro & Solyemez, 2000) by calculation of the real-axis intersections of the Nyquist plot.

In the present paper these results are generalized to a larger class of problems, an alternate proof is given via the parameter space approach, and a simple computational strategy is shown.

Consider the characteristic polynomial of a control system with the structure

$$P(s, q) = A_i(s)Q(s) + B_i(s), \quad i = 1, 2, \dots, N, \quad (1)$$

where $q = [q_0\ q_1 \dots q_\ell]^T$, $Q(s) = [1\ s\ \dots\ s^\ell]q$ and the index i represents different operating conditions of a plant.

As an example consider the design of a PID controller

$$\text{PID}(s) = \frac{K_I + K_P s + K_D s^2}{s} \quad (2)$$

for simultaneous stabilization of a plant family $G_i(s) = N_i(s)/D_i(s)$, $i = 1, 2, \dots, N$. The characteristic polynomial (1) is obtained by letting $A_i(s) = N_i(s)$, $B_i(s) = sD_i(s)$, $Q(s) = K_I + K_P s + K_D s^2$.

For each operating condition the set of all stabilizing q is determined and the set of all simultaneous stabilizers is the intersection of the N sets. The calculation of such intersection is not easy, since—except for trivial examples—the sets for each i are nonconvex (Ackermann, Bartlett, Kaesbauer, Sienel, & Steinhauser, 1993). Since we insist in exact boundaries, convex subsets or other approximations are avoided. The convex polygon result by Bhattacharyya and coworkers (Ho, Datta, & Bhattacharya, 1998; Datta, Ho, & Bhattacharya, 2000) is encouraging in the sense that nonconvex sets may have convex slices in particular directions. Then the intersection of convex polygons in a slice plane is easy.

In the present paper the problem is solved for a polynomial $Q(s)$ of arbitrary degree and with uncertain even or odd

part. This leads to the definition of singular frequencies in Section 2. In Section 3 the stability boundaries in form of a hyperplane for each singular frequency are derived. These hyperplanes divide the parameter space into a finite number of convex polyhedra. Then the stable ones must be sorted out. In Section 4 the case $\ell = 3$ is worked out in detail with a robust PID controller design as an example. Section 5 generalizes the result to σ-stability, where the real part of all roots of $P(s)$ must be smaller then $\sigma = \sigma_0$.

2. Singular frequencies

Consider polynomials (1) for one operating condition

$$P(s, q) = A(s)Q(s) + B(s). \tag{3}$$

For $s = j\omega$ all polynomial s are split into their real and imaginary part, i.e. (omitting the arguments)

$$P(j\omega, q) = R_P + jI_P$$

$$= (R_A + jI_A)(R_Q + jI_Q) + (R_B + jI_B). \tag{4}$$

The polynomial $P(s, q)$ has a root at $s = j\omega$ on the imaginary axis if and only if $R_P = 0$ and $I_P = 0$.

$$\begin{bmatrix} R_P \\ I_P \end{bmatrix} = \begin{bmatrix} R_A R_Q - I_A I_Q + R_B \\ R_A I_Q + I_A R_Q + I_B \end{bmatrix} = \begin{bmatrix} 0 \\ 0 \end{bmatrix} \tag{5}$$

written in detail as

$$R_Q = q_0 - q_2\omega^2 + q_4\omega^4 \mp \cdots$$

$$I_Q = q_1\omega - q_3\omega^3 + q_5\omega^5 \mp \dots .$$

Eq. (5) becomes

$$\begin{bmatrix} R_P \\ I_P \end{bmatrix} = \begin{bmatrix} R_A & -\omega^2 R_A & \omega^4 R_A & \dots \\ I_A & -\omega^2 I_A & \omega^4 I_A & \dots \end{bmatrix} \begin{bmatrix} q_0 \\ q_2 \\ q_4 \\ \vdots \end{bmatrix}$$

$$+ \omega \begin{bmatrix} -I_A & \omega^2 I_A & -\omega^4 I_A & \dots \\ R_A & -\omega^2 R_A & -\omega^4 R_A & \dots \end{bmatrix} \begin{bmatrix} q_1 \\ q_3 \\ q_5 \\ \vdots \end{bmatrix}$$

$$+ \begin{bmatrix} R_B \\ I_B \end{bmatrix} = \begin{bmatrix} 0 \\ 0 \end{bmatrix}. \tag{6}$$

Obviously, both matrices in Eq. (6) have rank 1. (The trivial case $A(s) \equiv 0$ is excluded here). For fixed I_Q Eq. (6) represents two parallel hyperplanes in the parameter space with coordinates $q_0, q_2, q_4, \dots$. The two hyperplanes become identical at real frequencies ω for which

$$g_R(\omega) = \det \begin{bmatrix} R_A & R_B - I_A I_Q \\ I_A & I_B + R_A I_Q \end{bmatrix} = 0. \tag{7}$$

$$g_R(\omega) = R_A(I_B + R_A I_Q) - I_A(R_B - I_A I_Q) = 0. \tag{8}$$

It is easily verified that $g_R(\omega)$ is ω times a polynomial in ω^2. Its degree results from the highest degree in ω^2 occurring among the products $R_A I_B$, $R_A^2 I_Q$, $I_A R_B$ and $I_A^2 R_Q$. Only the positive roots in ω^2 result in a real frequency ω. These real solutions ω_k, $(k = 1, 2, \dots, K)$ are defined as "singular frequencies".

Remark. A dual result is obtained by fixing R_Q. The singular frequencies are then $\omega = 0$ and the real roots of

$$g_I(\omega) = -I_A(I_B + I_A R_Q) - R_A(R_B + R_A R_Q) = 0. \tag{9}$$

The interpretation of Eq. (8) is that the root set of $P(s, q_0, q_2, q_4, \dots)$ can cross the imaginary axis only through the "holes" at the singular frequencies ω_k.

Example 1.

$$P(s) = (s - 1)(q_0 + q_2 s^2) + s^2 + s + 1$$

$$q_0 \in [-2, 0.1]$$

$$q_2 \in [0.1, 0.7].$$

Fig. 1 shows the two-parametric root set generated by gridding q_0 and q_2. It can cross the imaginary axis only through the hole $\omega_1 = \sqrt{2}$. This example also serves as a warning, that gridding of ω most likely will miss the value $\omega_1 = \sqrt{2}$.
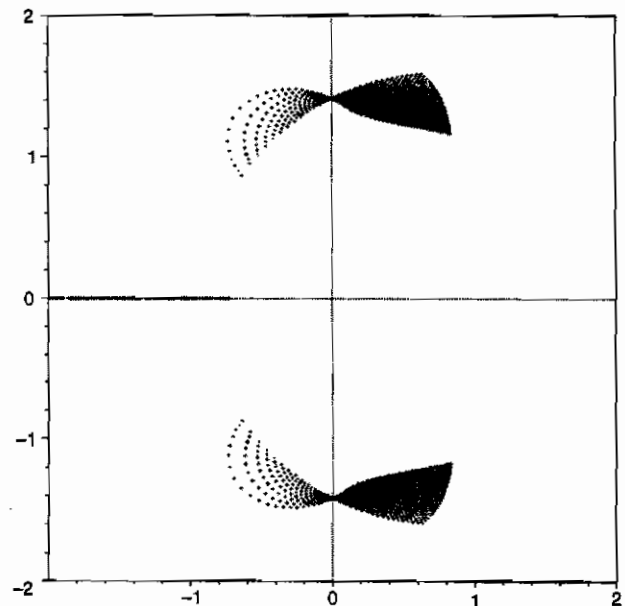

Fig. 1. The root cloud can cross the imaginary axis only through the hole $\omega_1 = \sqrt{2}$.

3. Stability boundaries in R_Q

Starting from a stable polynomial (3) there are three possibilities how a root can cross over the imaginary axis by variation of R_Q.

(a) a real root crosses at $s = 0$. For $\omega = 0$ we have $I_P = 0$ and the real root boundary (RRB) is obtained from

$$R_P(\omega = 0) = a_0 q_0 + b_0 = 0,$$

where $a_0 = A(0)$, $b_0 = B(0)$. The RRB is

$$q_0 = -b_0/a_0. \tag{10}$$

(b) a real root crosses at $s = \infty$. This infinite root boundary (IRB) is characterized by $p_n = 0$ in $P(s) = p_0 + p_1 s + \cdots + p_n s^n$. For the calculation of p_n let

$$A(s) = a_0 + a_1 s + \cdots + a_k s^k, \quad a_k \neq 0,$$

$$B(s) = b_0 + b_1 s + \cdots + b_m s^m, \quad b_m \neq 0.$$

Then

$$p_n = \begin{cases} a_k q_\ell & \text{for } m < k + \ell, \\ a_k q_\ell + b_m & \text{for } m = k + \ell, \\ b_m & \text{for } m > k + \ell. \end{cases}$$

In the R_Q-space the IRB is

$$q_\ell = \begin{cases} 0 & \text{for } m < k + \ell, \\ -b_m/a_k & \text{for } m = k + \ell, \\ \text{no boundary} & \text{for } m > k + \ell. \end{cases} \tag{11}$$

(c) a conjugate pair of roots crosses at one of the singular frequencies ω_k. These complex root boundaries (CRB) are obtained by substitution of ω_k into the first row of (5) (assuming $R_A \neq 0$) or second row (assuming $I_A \neq 0$). The first row becomes

$$R_P(\omega_k)$$
$$= R_A(\omega_k)R_Q(\omega_k) - I_A(\omega_k)I_Q(\omega_k) + R_B(\omega_k) = 0.$$

The CRB's are

$$R_Q(\omega_k) = [R_B(\omega_k) - I_A(\omega_k)I_Q(\omega_k)]/R_A(\omega_k),$$
$$k = 1, 2, \ldots, K. \tag{12}$$

For fixed I_Q Eq. (12) represents K hyperplanes in the parameter space of R_Q-coefficients.

In summary, roots of $P(s)$ cross the imaginary axis as R_Q crosses one of the hyperplanes (10), or (11) or one of the K hyperplanes (12). These hyperplanes divide the R_Q-space into a finite number of convex polyhedra. There remains the decision, which of these polyhedra are stable. This problem can be solved for example by testing one point in each polyhedron for stability.

4. Robust PID controller design

In this section $\ell = 2$ is chosen and the PID controller notation of (2) is used, i.e.

$$Q(s) = K_I + K_P s + K_D s^2. \tag{13}$$

Obviously, it is not essential that the controller has the denominator s. Any other fixed denominator can be multiplied with the plant denominator to form $B(s)$. Now $R_Q = K_I - K_D\omega^2$, and stable polygons in the (K_I, K_D)-plane for fixed K_P are sought. The hyperplanes become straight lines in the plane. The three types of stability boundaries lines are

(a) RRB $K_I = -b_0/a_0$,

(b) IRB

$$K_D = \begin{cases} 0 & \text{for } m < k + 2, \\ -b_m/a_k & \text{for } m = k + 2, \\ \text{no boundary} & \text{for } m > k + 2. \end{cases}$$

(c) CRB Singular frequencies are the real solutions of

$$g_R(\omega) = R_A(\omega)[I_B(\omega) + R_A(\omega)\omega K_P]$$
$$\quad - I_A(\omega)[R_B(\omega) - I_A(\omega)\omega K_P] = 0. \tag{14}$$

For each real solution a straight line is obtained

$$K_I - K_D\omega_k^2 = [R_B(\omega_k) - I_A(\omega_k)\omega_k K_P]/R_A(\omega_k).$$

In the (K_D, K_I)-plane these are lines with positive slopes ω_k^2.

Together with the RRB (zero slope in (K_D, K_I)-plane) and the IRB (infinite slope if $m < k + 2$) these lines divide the (K_D, K_I)-plane into a finite number of convex polygons. The polygons may also be open to infinity.

It remains to be determined, which of the polygons are stable. One possibility is to choose a testing point in each polygon and to check the stability of the polynomial. The resulting stability or instability property then applies to the entire polygon. This approach is suited for the interactive interpretation by the design engineer. Alternatively all intersection points of the straight lines are calculated. These intersections cut each lines into several line segments. Checking the center of the segment yields a polynomial with one or more roots on the imaginary axis. If all remaining roots are stable, then the segment is an active boundary. Otherwise the segment is omitted. The remaining segments form the boundary of the stable polygons. This second approach is more suited for automated calculation and plotting of the stability regions by the computer.

Example 2. Let $A(s) = -s^4 - 7s^3 - 2s + 1$ and $B(s) = s(s + 1)(s + 2)(s + 3)(s + 4)(s^2 + s + 1)$. The RRB for $s = 0$ is $K_I = 0$, the IRB for $s = \infty$ does not exist because $m = 7 > \ell + 2 = 6$.
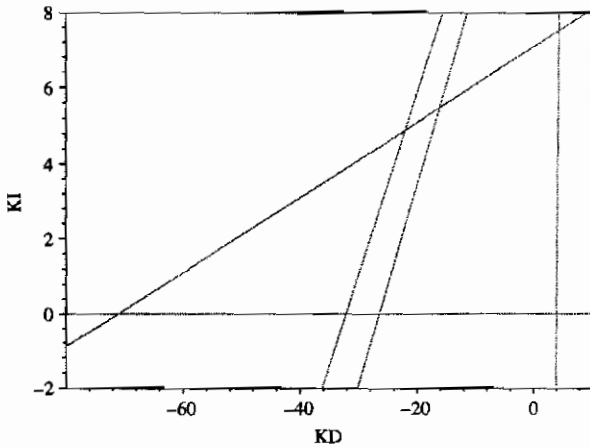
　　　　　　　　　　　J. Ackermann, D. Kaesbauer / Automatica 39 (2003) 937–943

Fig. 2. Root boundaries in the (K_D, K_I)-plane, $K_P = -4.4$.
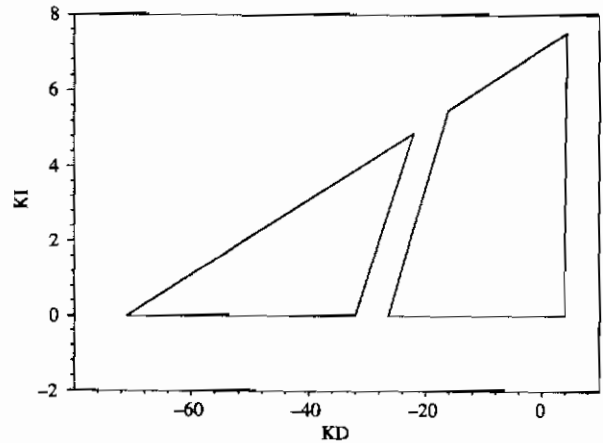

Fig. 3. Active boundaries in the (K_D, K_I)-plane, $K_P = -4.4$.

For the CRB we have to determine the singular frequencies ω_k^*. The polynomial (14) is

$$\omega^{10} + (31 + K_P)\omega^8 + (-579 + 49K_P)\omega^6$$

$$+ (730 - 30K_P)\omega^4) + (-257 + 4K_P)\omega^2 + 24 + K_P = 0.$$

The following table shows for $K_P = -4.4$ the singular frequencies (including 0) and the corresponding equations of the straight lines. Note that one zero of the polynomial is negative and does not yield a real ω.

singular frequency ω_k^*	straight line
0	$K_I = 0$
0.3156	$K_I = 0.01 K_D + 7.09$
0.695	$K_I = 0.48 K_D + 15.5$
0.730	$K_I = 0.53 K_D + 14.1$
4.13	$K_I = 17.1 K_D - 67.0$

Fig. 2 shows the RRB and the CRB (five straight lines) in the (K_D, K_I)-plane. Intersecting all lines with each other and testing the stability of the segment shows that the stability region splits in two polygons, a quadrangle and a triangle (Fig. 3).

A brute force approach for the calculation of stability regions in the (K_I, K_P, K_D)-space is to grid K_P and use a tomographic representation of the result. The 3D stability region is thereby represented as a family of convex polygons, see Fig. 4.

In order to get an orientation about interesting K_P-values one may form the discriminant of the polynomial (14), i.e. $dg_R(\Omega)/d\Omega = 0$, where $\Omega = \omega^2$.

The zeros of the discriminant divide the K_P-range into several segments such that the number of singular frequencies (resp. straight lines) is constant in each segment. Thus we can determine the range(s) of K_P for which stabilization by choice of K_D and K_I is possible.
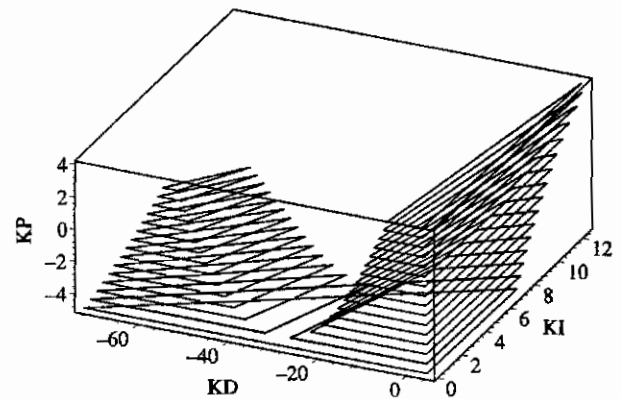

Fig. 4. 3D stability region, $K_P \in [-4.5, 4]$.

Starting at $-\infty$ the first stabilizing polygon (a triangle) arises at $K_P = -24$. At $K_P = 4.51$ the triangle splits into two polygons (a quadrangle and a triangle), see Fig. 4.), at $K_P = 4$ the triangle disappears and at $K_P = 6.15$ we arrive at the last stabilizing polygon. Thus a stabilization by choice of K_D and K_I is possible only in the interval $-24 < K_P < 6.15$. For $K_P < -4.51$ the triangle connects the two stability polygons of Fig. 4, such that the 3D stability region is simply connected. Fig. 4 illustrates that a nontrivial, nonconvex stability region has been represented by convex polygons in appropriately chosen slices.

In all other 2D cross sections the stability boundaries are curves, which require much more computation time.

A further drastic simplification is obtained, if we do not calculate the singular frequencies $\omega_k(K_P)$ for each grid point K_P by factorization of the polynomial (14). Instead we evaluate the inverse function $K_P(\omega)$, as it follows from the linear equation (14)

$$K_P(\omega^2) = \frac{I_A(\omega^2)R_B(\omega^2) - R_A(\omega^2)I_B(\omega^2)}{\omega[R_A(\omega^2)^2 + I_A(\omega^2)^2]}. \tag{15}$$

Now K_P is evaluated for a grid on ω. The singular frequencies ω_k for any fixed K_P can be determined from the
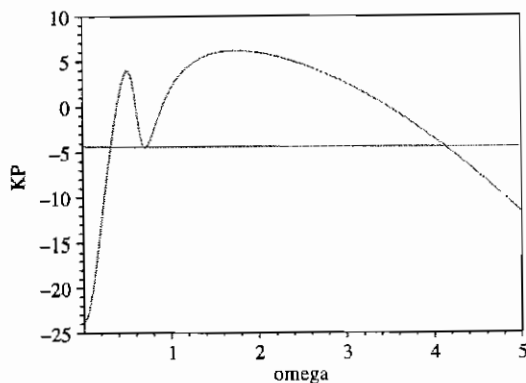
Fig. 5. K_P as function of ω.

graph. Fig. 5 illustrates this graph for Example 2. The line $K_P = -4.4$ intersects at the two closely neighboring frequencies 0.695 and 0.730 corresponding to two almost parallel lines in Fig. 2. The discriminant of Eq. (14) determines the maxima and minima of $K_P(\omega)$. A minimum occurs at the frequency $\omega = 0.713$ for $K_P = 4.51$, where the triangle and quadrangle unites to a large triangle.

For each candidate singular frequency $\omega^2 = \omega_k^2$ we obtain $K_P = K_P^*$ and the polygon for the ω_k's in the (K_P, K_I)-plane. The aggregation for an ω-grid generates the 3D stability region in (K_I, K_P, K_D)-space.

Consider now the problem that the operating range of a plant is described by several representatives $A(s) = A_i(s)$, $B = B_i(s)$, $i = 1, 2, \ldots, N$. The set of simultaneous stabilizers for this plant family is the intersection of the stability regions in (K_I, K_P, K_D)-space. For each fixed K_P the N convex polygons must be intersected.

Example 3 (Datta et al.). The plant $K/(1 + sT)^8$ with $K = 1$ should be simultaneously stabilized for $T = 0.5$ and $T = 1.5$ by a PID controller with transfer function (2). For $K_P = 0.35$ the intersection of the stabilizing regions is shown in Fig. 6. For example $K_D = 0.35, K_I = 0.091$ is a good centrally located choice for a simultaneous stabilizer. Note that for PID controllers the polynomial $B(s)$ contains the factor s from the denominator of the PID controller.

5. σ_0-stability boundaries

The result of the analysis so far is a description of the stable region in (K_I, K_P, K_D)-space by its boundaries in form of a family of polygons. Note that it is a "sharp" boundary in the sense that each point on the boundary yields a polynomial with roots on the imaginary axis. There remains the problem of choosing an appropriate controller from the set of admissible controllers. Typically this is done in a higher level optimization as a tradeoff with other design considerations. Nevertheless there may be a need for a "scalar" reduction of the admissible 3D solution set.
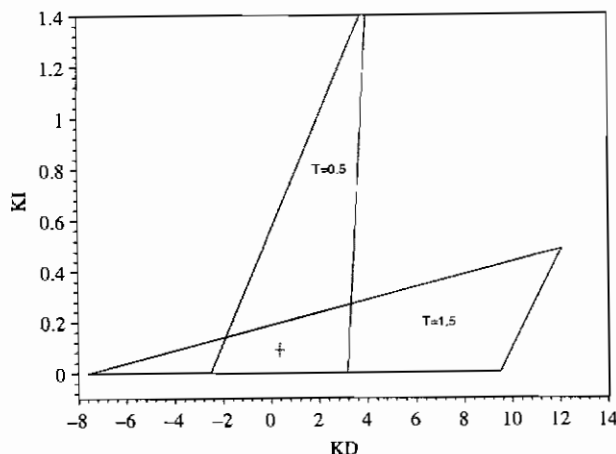

Fig. 6. Simultaneous stabilization for $T = 0.5$ and $T = 1.5$.

In terms of settling time, it is desirable to shift all eigenvalues to the left of a parallel to the imaginary axis with real part σ_0. This property of σ_0-stability is obtained by substituting s by $v + \sigma_0$ in Eq. (3), i.e.

$$P(v + \sigma_0, q) = A(v + \sigma_0)Q(v + \sigma_0) + B(v + \sigma_0). \quad (16)$$

The original polynomial (3) is σ_0-stable if and only if the new polynomial (14) in the complex variable v is Hurwitz-stable. The details are worked out here for the PID controller case.

Choosing σ_0-stability with $\sigma_0 < 0$ then the σ_0-stability region in the (K_D, K_I)-plane for fixed K_P is no loner bounded by polygons. In a transformed coordinate system, however, the nice geometric properties of convex polygons are recovered. Eq. (16) may be written as

$$A(v + \sigma_0)(K_I' + K_P'v + K_D'v^2) + B(v + \sigma_0) = 0$$

with

$$K_I' = K_I + \sigma_0 K_P + \sigma_0^2 K_P,$$

$$K_P' = K_p + 2\sigma_0 K_P,$$

$$K_D' = K_D.$$

For fixed K_P' the σ_0-stability regions are again bounded by convex polygons but now in the (K_D', K_I')-plane.

The linear transformation is always nonsingular, so it is possible to go back to the original parameters by the inverse transformation

$$K_I = K_I' - \sigma_0, K_P' + \sigma_0^2 K_D',$$

$$K_P = K_P' - 2\sigma_0 K_D',$$

$$K_D = K_D'.$$

Example 2 (continued). Choose $\sigma_0 = -0.1$ and $K_P = -4.4$. Fig. 7 shows the σ_0-stability region in the original
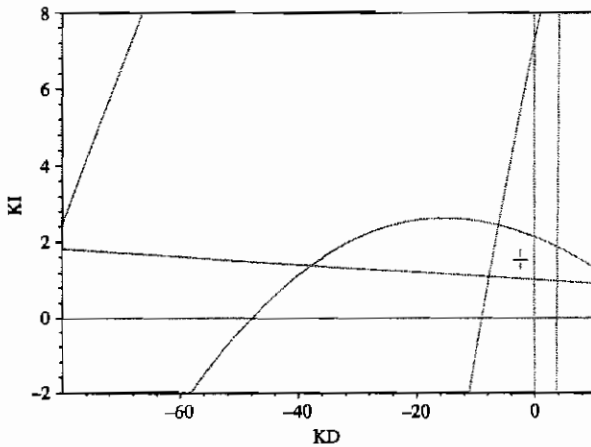
Fig. 7. σ_0-stability region in the (K_D, K_I)-plane, $\sigma_0 = -0.1$, $K_P = -4.4$.
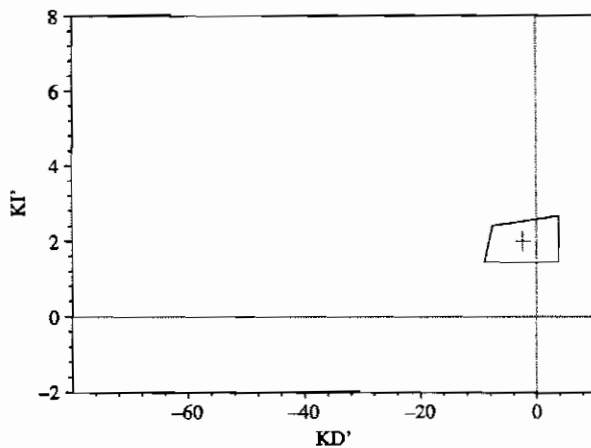

Fig. 8. σ_0-stability region in the (K_D', K_I')-plane, $\sigma_0 = -0.1$.

Fig. 9. σ_0-stabilizing PID parameters.

Fig. 10. Robustness w.r.t. time constant T and loop gain K.

(K_D, K_I)-plane. All straight lines become curves and the computation is much more involved. If we, however, choose the inclined (K_D', K_I') cross section plane with $K_P' = -4.4$ for the representation of the σ_0-stability region we obtain the simple convex polygon structure. The active boundaries are shown of Fig. 8. By comparison with Fig. 3 the shift from $\sigma = 0$ to $\sigma_0 = -0.1$ has removed the triangle, and the quadrangle is much smaller now. An appropriate choice is $K_D' = -2.4$ and $K_I' = 2$. Back transformation gives finally $K_D = -2.4$, $K_P = -4.88$, $K_I = 1.54$.

Example 3 (continued). Let $T = 1$, $K = 1$. Datta arrives at $\sigma_0 = -0.103$ as a good solution to the controller fragility problem. Now let $\sigma_0 = -0.25$. Then Fig. 9 shows the set of all σ_0-stabilizing PID parameters. Choosing the center of gravity of a large triangle leads to $K_I' = 0.029$, $K_P' = 0.918$, $K_D' = 0.635$ and

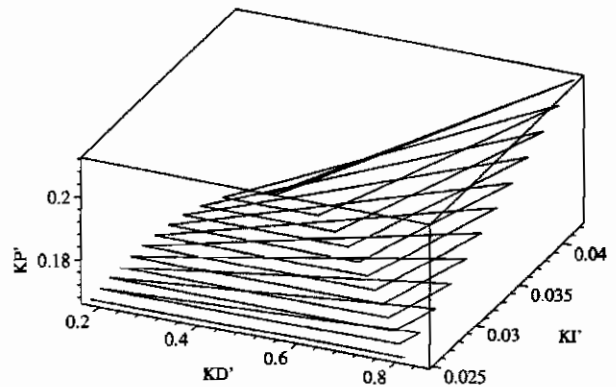$$K_I = 0.118, \quad K_P = 0.516, \quad K_D = 0.635$$

and $\sigma = -0.27$.

In this example we can determine the optimal σ_0 exactly. For this purpose we place four poles at $s = \sigma_0$ and optimize σ_0. The choice of $K_P = K_D = 256/729 \approx 0.35$, $K_I = 1792/19683 \approx 0.091$ gives four poles at $s = -1/3$. The quadruple eigenvalue at $s = -1/3$ leads to a high local sensitivity. However, the robustness analysis for varying time constant T and loop gain K in Fig. 10 shows a good distance of the nominal point $T = 1$, $K = 1$ from the Hurwitz stability boundary. This figure also verifies Hurwitz stability for the entire interval $0.5 < T < 1.5$, in the controller construction only the end points have been considered. Obviously T is a convex direction in the nonconvex region although T enters polynomially into the characteristic polynomial coefficients.

6. Conclusion

For a polynomial $P(s, q) = A(s)Q(s) + B(s)$ it has been shown that the stability region in the space of the even part of $Q(j\omega)$ may be exactly represented by a family of convex polyhedra for constant imaginary part of $Q(j\omega)$. In control system design the $Q(s)$ is a numerator or denominator term

of the controller, for example the parameters of a PID controller. The simultaneous design for a plant family $A = A_i$, $B = B_i$, $i = 1, 2, \ldots$, then reduces to finding the intersection of convex polygons. Settling time requirements for the negative real part of all roots of $P(s, q)$ can be treated by a linear coordinate transformation.

Some nontrivial connections with other approaches are topics for future research, e.g. the fact, that a two-parametric family of root loci crosses the imaginary axis only at singular frequencies.

The paper also contains results on the efficient calculation of the stable polygons. Further work will be needed to marry the simple calculation of nonconvex 3D objects with computer graphic methods for analysis and design of robust control systems.

References

Ackermann, J., Bartlett, A., Kaesbauer, D., Sienel, W., & Steinhauser, R. (1993). *Robust control: Systems with uncertain physical parameters.* London: Springer.

Datta, A., Ho, A., & Bhattacharya, S. (2000). *Structure and synthesis of PID controllers.* London: Springer.

Ho, M., Datta, A., & Bhattacharya, S. (1998). Design of P, PI and PID controller for interval plants. In *Proceedings of the American control conference*, Philadelphia (pp. 2496–2501).

Munro, N., & Solycmez, M.T. (2000). Fast calculation of stabilizing PID controllers for uncertain parameter systems. In *Proceedings of 3rd IFAC symposium on robust control design*, Prague, Czech Republic, 2000.

Juergen Ackermann received the Dipl.-Ing. and Dr.-Ing. degrees from the Technical University Darmstadt, the M.S. degree from the University of California, Berkeley, and the Habilitation degree from the Technical University of Munich, Germany. Since 1962 he has been with the German Aerospace Research Establishment (DLR), Oberpfaffenhofen, Germany. From 1974 to 2001 he was Director of the Institute of Robotics and Mechatronics. He is also Adjunct Professor at the Technical University of Munich. His main research interests include parametric robust control and vehicle steering applications. He is author of books on Sampled-Data Control Systems (New York: Springer-Verlag, 1985) and Robust Control (New York: Springer-Verlag, 2002). Dr. Ackermann is a Fellow of IEEE and recipient of the Nathaniel-Nichols Medal from IFAC and Hendrik-Bode-Lecture Prize from the IEEE Control Systems Society.

Dieter Kaesbauer was born in Landshut, Germany, in 1944. He received the M.S. degree in mathematics from the Technical University of Munich, in 1970, and the Dr. techn. degree from the Technical University of Graz, in 1986. Since 1971 he worked as a research scientist in the control group of the Institute of Robotics and Mechatronics at the German Aerospace Research Establishment (DLR), Oberpfaffenhofen, Germany. His research interests are in robustness analysis and control systems design.